

# Synthesis of Enaminothiones and Computational Investigation of Intramolecular Hydrogen Bonding Strength and Substituent Effects Using DFT, QTAIM, and NCI.

Firas A. Nawar<sup>\*1</sup>, Bahjat A. Saeed<sup>2</sup>, Poul Erik Hansen<sup>3</sup>

<sup>1</sup>Department of Chemistry, College of Education, University of Sumer, Dhi-Qar, Iraq. ORCID: 0009-0001-1069-198X.

<sup>2</sup>Department of Chemistry, College of Education for Pure Sciences, University of Basrah, Basrah 61001, Iraq.

<sup>3</sup>Department of Science and Environment, Roskilde University, Roskilde, Denmark. ORCID: 0000-0003-4751-9910.

\* [rasalattabi57@gmail.com](mailto:rasalattabi57@gmail.com)

## Abstract

Enaminothiones were prepared, and the effects of aromatic and aliphatic substitutions on the strength of intramolecular hydrogen bonds were studied via DFT calculations ( $\omega$ B97XD/6-311++G(d,p)), QTAIM and NCI analyses. The results showed that aromatic substitutions enhance the strength of hydrogen bonds, as they result in shorter S...N distances, higher electron density ( $\rho$ BCP), and stronger hydrogen bond energy (35.80–36.69 kJ/mol) than those of aliphatic compounds. NMR measurements confirmed this with greater chemical shifts of the NH proton in aromatic compounds (15.74–15.88 ppm), and NCI analysis revealed more negative  $\text{sign}(\lambda_2)\rho$  values, indicating stronger bonding. This study confirms the role of substitutions in modifying the strength of hydrogen bonds, which may have an impact on the design of pharmaceutical compounds and chemically active materials.

**Keywords:** Enaminothiones, DFT, NCI, QTAIM

## تحضير الإينامينوثيونات ودراسة حاسوبية لقوة الروابط الهيدروجينية الضمنية وتأثير المعوضات باستخدام نظرية دالية الكثافة الوظيفية (DFT) وتحليل نظرية الذرات في الجزيئات (QTAIM) وتفاعلات غير التساهمية (NCI)

فiras عباس نوار<sup>1</sup>, بهجت علي سعيد<sup>2</sup>, بول اريك هانسن<sup>3</sup>

<sup>1</sup>قسم الكيمياء، كلية التربية، جامعة سومر، ذي قار، العراق

<sup>2</sup>قسم الكيمياء، كلية التربية للعلوم الصرفة، جامعة البصرة، البصرة، العراق

<sup>3</sup>قسم العلوم والبيئة، جامعة روسكيلدا، روسكيلدا، الدانمارك

## الخلاصة

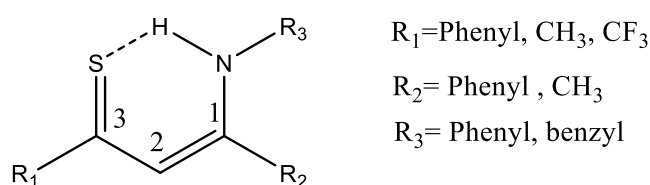
تم تحضير مركبات الإينامينوثيونات، وتمت دراسة تأثير المعوضات الأروماتية والأليفاتية على قوة الروابط الهيدروجينية الضمنية باستخدام حسابات نظرية الكثافة الوظيفية (DFT) بطريقة ( $\omega$ B97XD/6-311++G(d,p))، بالإضافة إلى تحليلات QTAIM و NCI. أظهرت النتائج أن المعوضات الأروماتية تعزز من قوة الروابط الهيدروجينية، حيث تؤدي إلى تقصير المسافة بين ذرتي الكبريت والنيتروجين (S...N)، وزيادة كثافة الإلكترونات عند نقطة الاتصال ( $\rho$ BCP)، وطاقة رابطة هيدروجينية أعلى (تتراوح بين 35.80 و 36.69 كيلوجول/مول) مقارنةً بالمركبات الأليفاتية. أكدت قياسات الرنين المغناطيسي النووي (NMR) هذه النتائج من خلال التغير الأكبر في الإزاحة الكيميائية لبروتون NH في المركبات الأروماتية (من 15.74 إلى 15.88 جزء في المليون). كما أظهر تحليل NCI قيماً أكثر سلبية لـ  $\text{sign}(\lambda_2)\rho$ ، مما يدل على روابط أقوى. تؤكد هذه الدراسة دور المعوضات في تعديل قوة الروابط الهيدروجينية، مما قد يؤثر على تصميم المركبات الدوائية والمواد الكيميائية النشطة، ويسهم في تطوير مركبات ذات فعالية بيولوجية أو كيميائية محسنة.

## 1. Introduction

Enaminothiones are a unique class of heterocyclic compounds of conjugated sulfur-containing organic compounds characterized by the presence of an extended (HN-C-C=C-C=S) moiety conjugated with a  $\pi$ -system. Enaminothiones increase electron density delocalization, which in turn affects their acidity, nucleophilicity, and hydrogen bonding activity [1]. The presence of a vinylogous extension C=C influences the chemical reactivity of enaminothiones by stabilizing resonance-assisted hydrogen bonding (RAHB) and promoting electronic delocalization between several atoms [2]. Because hydrogen bonds play a significant role in chemical reactions, biological phenomena, relationships within condensed phases, crystal engineering, and other fields, predicting their properties is one of the most significant scientific challenges [3]. Because amines are very important in pharmacology [4], studying the effects of hydrogen bonds in this research could help improve the design and effectiveness of compounds of this class. This could lead to more medical and pharmaceutical uses for these patients. A recent study [5] revealed that compounds derived from enamines, such as enaminothiones, possess unique electronic and optical properties that can be improved by tuning the molecular structure and modifying hydrogen bonds.

Hydrogen bonding is typically characterized as a weak contact between an electronegative proton donor and an electronegative proton acceptor. Significant work has been devoted to comprehending unusual hydrogen bonding [6]. For instance: C-H...X [7], X-H...C [8]. The stabilization energy of intermolecular hydrogen bonding is the difference between the energy of the complex and that of the isolated molecules [9]. An approach of this kind cannot be considered for intramolecular systems, and there is no direct method for calculating the energy of the H-bonds that are present within the molecules themselves [10]. Nevertheless, such relationships are typically satisfied in the context of homogeneous samples. For instance, in O-H...O systems, the association between the O-H bond length and H...O distance has frequently been examined [11]. The energy of the intramolecular hydrogen bond in this study was calculated using the Espinosa formula [12]. The strength of the hydrogen bond in the intramolecular hydrogen-bonded systems was evaluated via AIM analysis, and a significant correlation between the hydrogen bond H...S length and topological properties of the bond critical points ( $\rho$ BCP) were determined. The bond critical point (BCP) is a good tool for estimating the strength of hydrogen bonds [13].

The topological characteristics were examined via Bader's atoms in molecules (AIM) theory [14] to determine the hydrogen bond's bond critical point (BCP) and hydrogen bond energy. Scheme 1 illustrates the enaminothione compounds and their substituents employed as a model to investigate the strength of the intramolecular hydrogen bond in this work.



**Scheme -1** Enaminothione ring with numbering carbon atoms and their substituents

The geometric parameters, length of the NH, S...H hydrogen bond length and S...N distance are the primary geometric characteristics that characterize the strength of the NH...S hydrogen bonds

[15]. The studied compounds were optimized via density functional theory (DFT) at the  $\omega$ B97XD level, and the basis set was 6-311++G(d,p) to obtain the total energy and geometric parameters [16]. The synthesized compounds were identified as enriched by NMR spectroscopy, which revealed the chemical shift of the NH proton downfield. Since the NCI approach can overcome some of the drawbacks of the AIM theory and offers a more comprehensive explanation of noncovalent bonding (hydrogen bonding), it has been utilized recently to investigate a variety of noncovalent interactions [17]. The synthesis of sulfur ylides and other chemicals has potential applications in industry, labs, pharmaceutical businesses, medication production, clinical use, medicinal chemistry, and agrochemistry [18]. However, there has not been as much research done on the characteristics of N-H...S systems. The molecular structure can be ascertained by considering the hydrogen bond strength, heavy atom distance, XH chemical shift, XH stretching frequency, and XH bond length [19-20]. This work aims to identify the strength of the intramolecular hydrogen bond in enaminothione compounds and to assess the influence of aromatic and aliphatic substituents on the nitrogen atom via NCI and AIM calculations. These computations yield significant insights into the strength and stability of the hydrogen bonding of these molecules [21].

## 2. Computational details

The computations in this investigation were conducted using the Gaussian 16 suite of programs [22]. Geometry optimizations were conducted at the  $\omega$ B97XD/6-311G++(d,p) level of theory. Optimizations were conducted for compounds exhibiting intramolecular hydrogen bonds (NH...S). This study investigated the intramolecular hydrogen bonds in enaminothione derivatives via the Bader theory of atoms in molecules (AIM) [23]. The AIM approach was expanded and integrated into Gaussian software by Cioslowski [24]. This analysis was conducted because the electronic density at the bond critical point (BCP), denoted as  $\rho_{\text{BCP}}$ , and its Laplacian, represented as  $\nabla^2\rho_{\text{BCP}}$ , are valuable metrics for assessing the relative strength of hydrogen bonding [25]. To assess the hydrogen bond energy within a molecule, the equation provided by Espinosa *et al.* [26] was used. On the basis of the attributes of the electron density distribution in the BCP.

NCI calculations were conducted via DFT with the  $\omega$ B97XD method and the 6-311++G(d,p) basis set. Reduced density gradient (RDG) graphs were produced with the Multiwfn program version 3.8. [27] This software was employed for the analysis of noncovalent interactions (NCIs), hole-electron dynamics, and excitation parameters. The outcomes of the noncovalent interaction (NCI) analysis were depicted via visual molecular dynamics (VMD) software, version 1.9.3. This process results in the generation of isosurfaces [28].

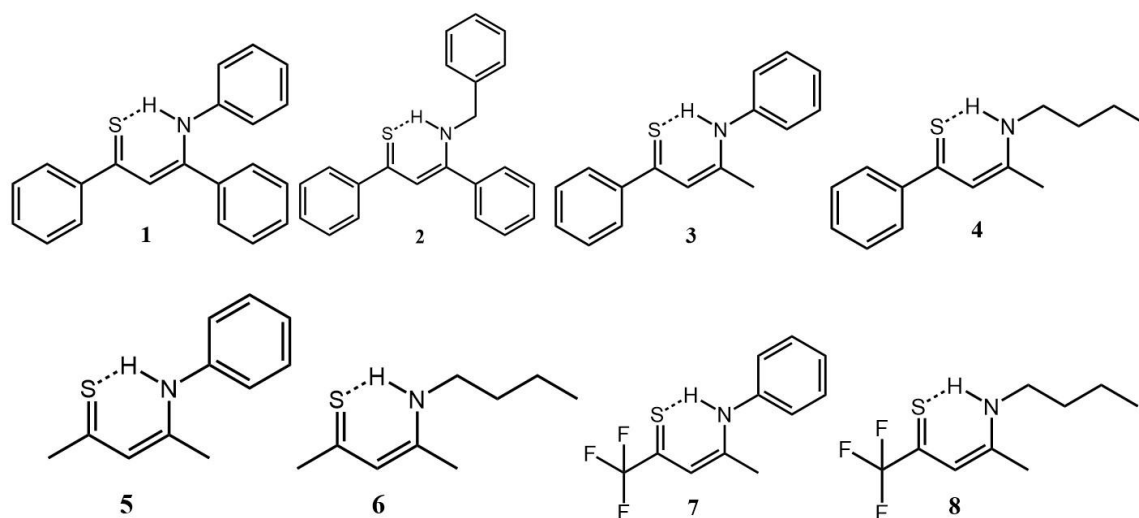
## 3. Results and discussion

### 3.1 $^1\text{H}$ and $^{13}\text{C}$ NMR spectroscopy

The results revealed a broad and high chemical shift signal of the NH proton within the range of 14.13–15.88 ppm, as shown in Table 1 and Scheme 2. The NH chemical shifts of the enaminothione compounds (1, 3, 5, and 7) with aromatic substituents, such as the phenyl ring on the nitrogen atom, ranged from 15.74 to 15.88 ppm. The clear effect of electron withdrawing in these systems on chemical shifts may account for the slightly different NH chemical shifts observed in these systems. Aliphatic substituents in compounds 2, 4, 6, and 8, such as butylamine and benzylamine, resulted in reduced chemical shifts between 14.13 and 14.77 ppm. Their effect on the electron density directed

at the nitrogen atom decreases the partial positive charge on the NH proton, leading to a reduced chemical shift [29]. The NH chemical shift values in the enaminothiones are close to the values observed in the enamines, indicating a similar hydrogen bonding effect in both cases [30]. The observed variations in the NH chemical shifts can be explained by both resonance and inductive effects of the N-substituents. Aromatic groups (e.g., phenyl) withdraw electron density via resonance and inductive effects, increasing the deshielding of the NH proton and leading to a downfield shift (~15.8 ppm). In contrast, aliphatic substituents such as butyl or benzyl groups donate electron density (+I effect), reducing NH deshielding and weakening hydrogen bonding, resulting in lower shifts (~14.1–14.7 ppm). Even though compounds 1 and 2 share a phenyl ring, it is interesting to note that compound 2 has a smaller NH shift. This is because the steric hindrance of the benzyl group probably alters and weakens the hydrogen bond geometry. Thus, the unusual chemical shift of compound 2 can be explained by both steric and electronic processes.

The experimental  $^{13}\text{C}$  NMR spectra of the enaminothiones analyzed in Table 1 revealed three distinct types of signals: C-3 (C=S) was observed within the range of 180.3–207.4 ppm, C-1 (C-N) was observed within 161.4–168 ppm, and C-2 (vinylic carbon) was observed within 111.2–113.8 ppm in the chelating ring. The C-1, C-2 and C-3 atoms form a chelated ring system that has the intramolecular hydrogen bond NH...S. The quaternary carbons are easy to identify because of their higher chemical shifts and lower intensity signals resulting from longer relaxation times and reduced Overhauser enhancement [31].



**Schem -2** Synthesized enaminothione structures of the compounds studied from 1 to 8.

**Table 1**-Experimental  $^1\text{H}$  and  $^{13}\text{C}$  chemical shifts (ppm) obtained at 296 K in  $\text{CDCl}_3$ , with TMS used as an internal reference.

compounds	$\delta\text{NH}$	$\delta\text{CH}$ vinylic	$\delta\text{C-1}$	$\delta\text{C-2}$	$\delta\text{C-3}$
1	15.74	6.76	161.4	113.6	205.9
2	14.77	6.56	166.6	112.3	202.9
3	15.88	6.65	164	113.3	203.6
4	14.37	6.52	166	112.9	199.7
5	15.55	6.28	163.6	113.8	207.4
6	14.13	5.99	164.7	113	201.7
7	15.81	6.81	167.7	111.2	184.3
8	14.47	6.60	168	111.9	180.3

Notably, the effect of the substituents on carbon atoms C-1 and C-3 did not clearly affect the strength of the intramolecular hydrogen bond because of the balance in the effects of the aliphatic and aromatic groups on the positions of those atoms. Therefore, the study was limited to the effect of the substituents on the nitrogen in the chelated ring, as those substituents clearly affect the strength and stability of the hydrogen bond.

### 3.2 Hydrogen bond energy in enaminothione

A method for the calculation of the intramolecular hydrogen bond (HB) energy (EHB) by Vbcp at the bond critical point as an approach for enaminothione compounds has been used for compounds with resonance-assisted hydrogen bonding (RAHB) [32]. Jabłoński's [33] comprehensive overview highlights the extensive research on intramolecular hydrogen bond strength. Espinosa proposed one indirect method, which will be the focus of our attention. Espinosa's method (EM) employs the topology of electronic density, particularly the correlation between the potential electron energy density at the bond critical point,  $V(\text{rbcp})$ , as shown in Table 3, related to a specific hydrogen bond and the corresponding energy, as indicated by the empirical expression [26].

$$E_{\text{intraHB}} \approx E_{\text{HB}} = 1/2 V(\text{rbcp})$$

Estimations derived from local parameters, particularly the S...N distance, may produce more reliable outcomes, as they are directly associated with the hydrogen bond and its localized interactions [34]. The existing compounds are very appropriate for examining the correlation between X...Y distances and hydrogen bond strength. Recently, research has shown that the introduction of electron-donating groups such as N,N-diethylamino significantly affects the distribution of electron density in a molecule, which may enhance or weaken the strength of hydrogen bonds [5]. Table 2 shows the geometric characteristics and energy calculations of the studied compounds.

**Table 2-** Geometric parameters calculated in <sup>a</sup>(Å), <sup>b</sup> $E_{HB}$  calculated in (kJ.mol<sup>-1</sup>) and total energy ZPE calculated in (Hartree)<sup>a</sup>.

Compounds	H...S (Å)	S...N (Å)	$E_{HB}$ (kJ.mol <sup>-1</sup> )	Total Energy ZPE (Hartree)
1	2.1060	3.0023	35.80	1263.32536
2	2.1305	3.0129	33.66	1302.63851
3	2.0971	2.9957	36.69	1071.61280
4	2.1241	3.0086	34.09	997.838607
5	2.103	3.0007	35.96	879.900282
6	2.1155	3.0116	34.67	806.127755
7	2.1120	2.9994	35.17	1177.63695
8	2.1215	3.0134	34.27	1103.86423

<sup>a</sup> The functional used is  $\omega$ B97XD, and the basis set is 6-311++G(d,p).

<sup>b</sup> $E_{HB}$  from the potential energy density at its bond critical point ( $V_{BCP}$ ).

A correlation between the hydrogen bond energy and the S...N distance for enaminothion compounds 1–8 is depicted in Fig. 1. Compared between the hydrogen bond energies of aliphatic and aromatic substituents. The aromatic substituents of compounds 1, 3, 5 and 7 (red dots) presented stronger hydrogen bonds and shorter S...N distances, whereas the aliphatic substituents of compounds 2, 4, 6, and 8 (red circles) presented weaker hydrogen bonds and larger S...N distances. Compared with other intramolecular HBs, the donor–acceptor distance in strong hydrogen bonds is 2.06–2.7 Å for the NH...N intramolecular systems and 2.5–2.6 Å for NH...O  $\beta$ -enaminones [35]. The S...N distance varies between 2.99 and 3.01 Å, according to the data in Table 2. Sulfur differs from the aforementioned materials because it is larger in size, more polarizable, and less electronegative than nitrogen and oxygen. This makes its geometric structure less rigid, has a longer S...N distance and is more flexible, which lowers the hydrogen bond energy. Every hydrogen bond is classified as part of the moderately strong hydrogen bond class 33.66--35.96 (kJ.mol<sup>-1</sup>).

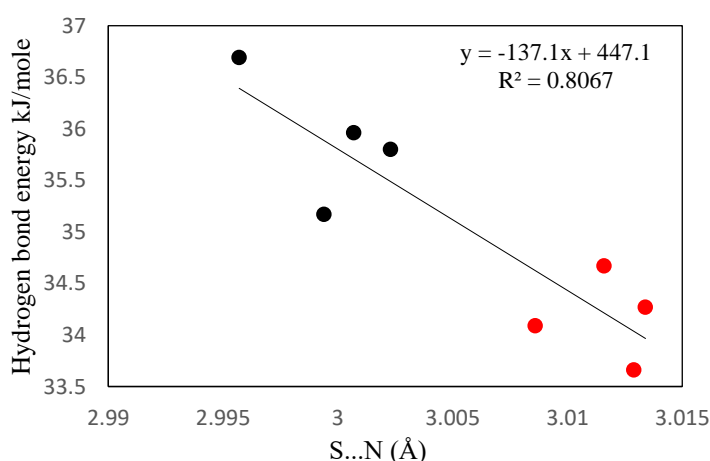


**Figure-1** Calculated HB energy in kJ.mol<sup>-1</sup> vs the calculated S...N distance in Å. (Red circles refer to aliphatic substituents, and black circles refer to aromatic substituents).

### 3.3 Atoms in molecules (AIM) calculations.

The quantum theory of atoms in molecules (QTAIM) is used to examine the properties of interatomic interactions [36]. The compounds examined in Table 3 have positive bond critical points  $\rho_{\text{BCP}}$  and Laplacian electron density  $\nabla^2\rho_{\text{BCP}}$  values, which suggests the existence of noncovalent bonding characteristics such as hydrogen bonding [37]. All of the compounds H... S bonds have a low  $\rho_{\text{BCP}}$  and  $\nabla^2\rho_{\text{BCP}} > 0$ . These are characteristics of interactions that take place in a closed shell interaction [38].

According to Rozas [39],  $\rho_{\text{BCP}} > 0$  and  $\nabla^2\rho_{\text{BCP}} > 0$  indicate medium H-bond strength (12.0 kcal/mole  $<$  EHB  $<$  24.0 kcal/mole). In the current systems, a medium hydrogen bond strength (33.66–36–69 kcal/mole) is indicated by the Laplacian at  $\nabla^2\rho_{\text{BCP}}$ . Through the examination of energy values derived from DFT calculations and Bader theory in various systems with different substituents, it has been noted that these systems have convergent energy values at intermediate hydrogen bond strengths. The potential hydrogen bond energy density ( $V_{\text{BCP}}$ ) values are shown in Table 3.

**Table 3-** The topological parameters (electronic densities  $\rho$  (in  $e/a_0^3$ ) and Laplacians of electronic densities  $\nabla^2\rho$  (in  $e/a_0^5$ ) and  $V_{\text{BCP}}$  for BCPs of H... S of the NH... S bridge calculated at the  $\omega\text{B97XD}/6\text{-}311\text{++G}$  (d,p) level of theory.

Molecules	$\rho_{\text{BCP}}$	$\nabla^2\rho_{\text{BCP}}$	$V(\mathbf{r}_{\text{BCP}})$
1	0.0376	0.0679	-0.0272
2	0.0357	0.0687	-0.0256
3	0.0384	0.0678	-0.0279
4	0.0362	0.0686	-0.0259
5	0.0379	0.0673	-0.0273
6	0.0367	0.0681	-0.0264
7	0.0371	0.0681	-0.0267
8	0.0362	0.0687	-0.0261

There is a strong relationship between the geometrical and topological characteristics of the species under study. The distance and electron density of hydrogen bonding H...S interactions exhibit linear correlations ( $R^2=0.99$ ); as shown in Fig. 2, the  $\rho_{\text{BCP}}$  increased as the bond length S...H decreased. The aromatic substituents of compounds 1, 3, 5, and 7 presented higher  $\rho_{\text{BCP}}$  values and shorter hydrogen bond S...H lengths (black circles), whereas the aliphatic substituents of compounds 2, 4, 6, and 8 (red dots) presented lower  $\rho_{\text{BCP}}$  values and longer hydrogen bond S...H lengths, indicating that the hydrogen bond strength of aromatic substituents is stronger than the hydrogen bond strength in the presence of aliphatic substituents in the studied compounds. The inverse relationship indicates that the  $\rho_{\text{H...S}}$  values are essential for evaluating the strength of hydrogen bonds in the studied systems.

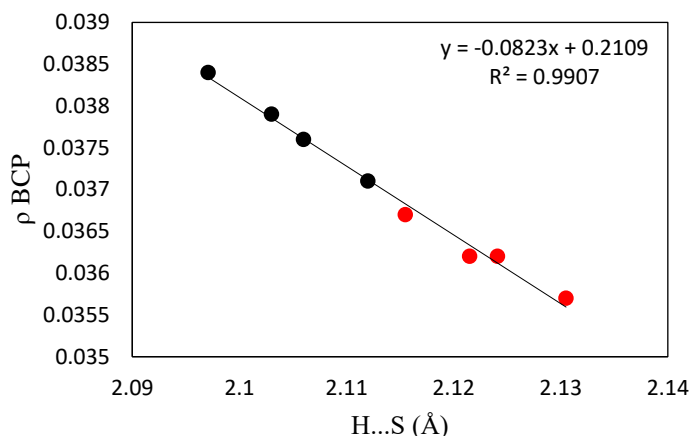


**Figure -2** The correlation between  $\rho_{BCP}$  and H... S hydrogen bond length (Å) for the enaminothion compounds. (Red circles refer to aliphatic substituents, and black circles refer to aromatic substituents).

### 3.4 Noncovalent interaction (NCI) calculations

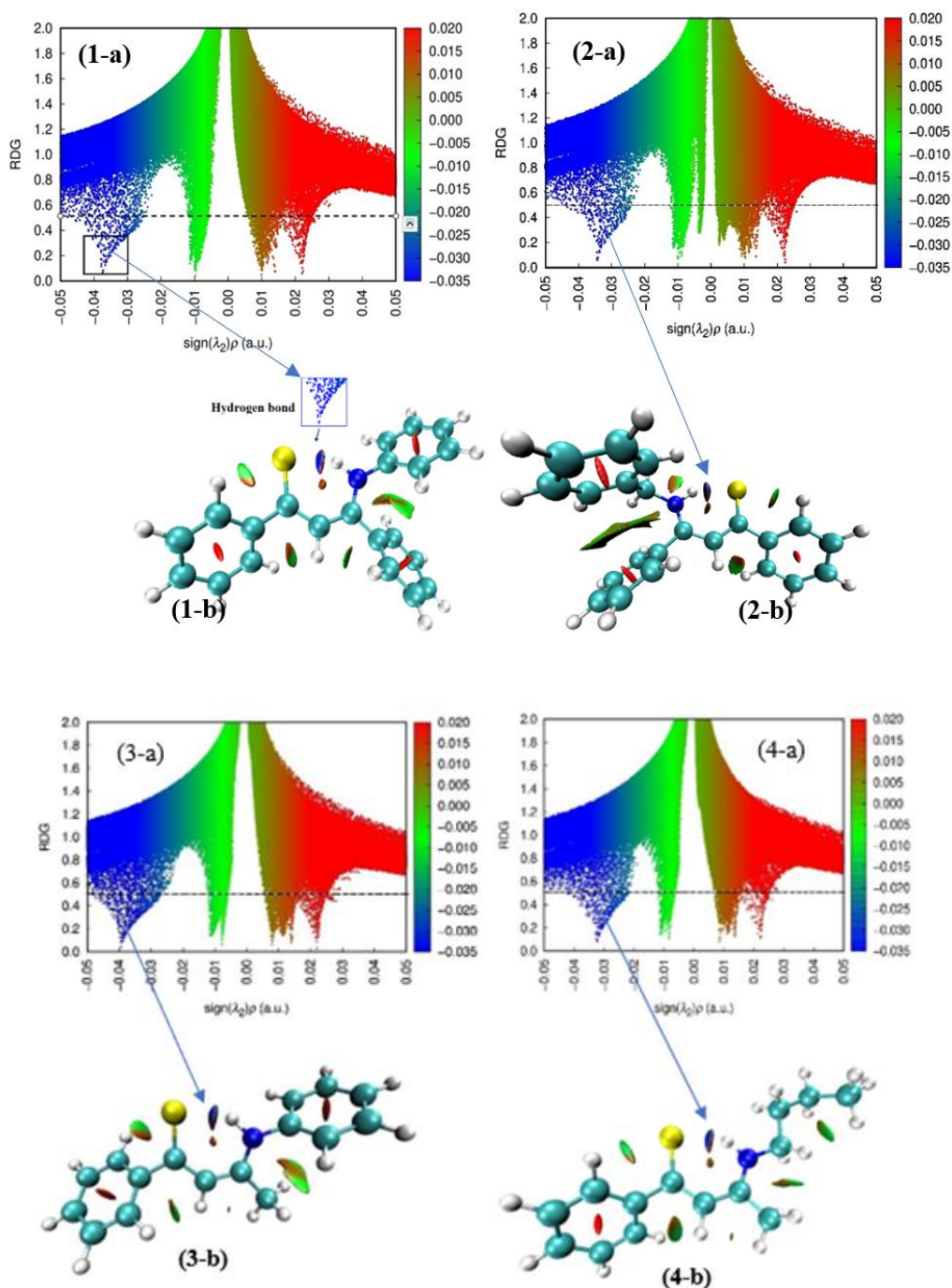
The noncovalent contact (NCI) method is a suitable approach for studying hydrogen bonding, which is a type of weak noncovalent contact [40]. The reduced density gradient methodology is a prominent topological approach that provides techniques for detecting and displaying noncovalent interactions (NCIs), which complements the current QTAIM method. It can be efficiently employed to examine and illustrate several types of noncovalent interactions, including hydrogen bonds, steric conflicts, and van der Waals interactions [41]. The process of identifying noncovalent interactions requires analyzing the electron density and its derivatives to locate the specific locations where these interactions take place precisely. This work enables the creation of graphical representations that depict these interactions. The NCI index is founded on the correlation between the electron density  $\rho(r)$  of the hydrogen bond and the reduced density gradient and is defined as follows [42]:

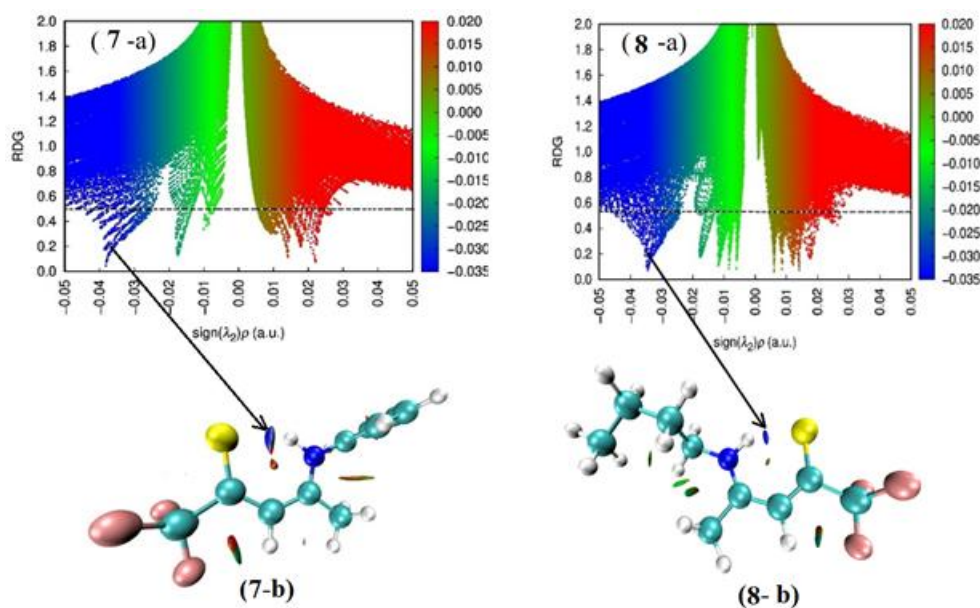
$$s = \frac{1}{2(3\pi^2)^{1/3}} \frac{|\nabla\rho|}{\rho^{4/3}}$$

It enables the visualization of isosurfaces in a reduced density gradient at low densities to elucidate the position and characteristics of noncovalent interactions in three-dimensional space [43]. This approach has recently been employed to investigate several forms of noncovalent interactions, as it can surmount certain constraints of the AIM theory, thereby offering a more comprehensive depiction of noncovalent bonding [17], [44]. Figure 3 shows the NCI isosurfaces and plots of the reduced density gradient, with strong attractive interactions depicted in blue corresponding to hydrogen bonds in the N-H...S bridge, weak interactions in green, and repulsive interactions in red. These images clearly demonstrate the characteristic intramolecular S...H interactions of varying-strength hydrogen bonding.

Fig. 3 shows that the compounds (1a, 3a, 5a, and 7a) contained aromatic substituents on the nitrogen atom, as shown in the RDG plots. There is a spike at a high density of the more negative values of  $\text{sign}(\lambda_2)\rho$  in blue at a density close to -0.04 a.u. corresponds to a stronger H-bond in the NH...S bridge. This is supported by the presence of 3D isosurfaces (Figures 1b, 3b, 5b, 7b) in which the disk lies between the proton of the amino group as a hydrogen donor and the sulfur atom of the

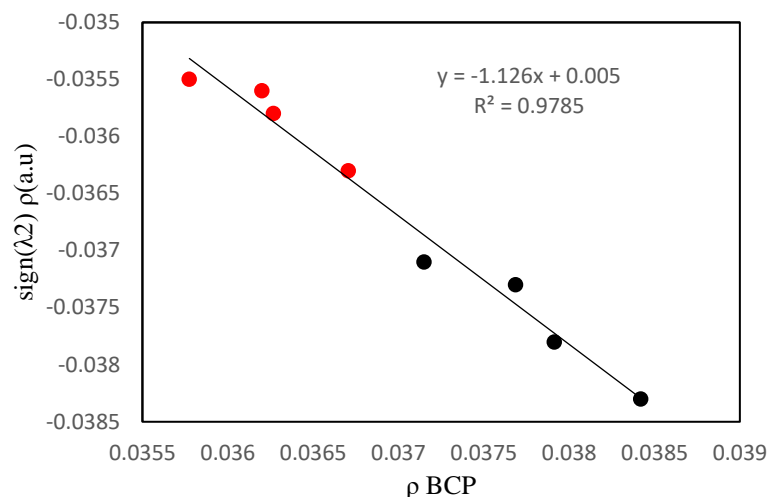
C=S group as an acceptor. Compared with the figures (2a, 4a, 6a, 8a), which represent compounds containing aliphatic substituents on the nitrogen atom, these compounds presented blue spikes in RDG plots closer to -0.03 a.u., which was less negative than aromatic substituents. The less negative values of  $\text{sign}(\lambda_2)\rho$  reflect less attractive forces of H-bonds in the NH...S bridge [41]. The presence of 3D isosurfaces in Figures 2b, 4b, 6b, and 8b, which contain aliphatic substituents, further support that the light blue disc lies between the proton of the amino group and the sulfur. In addition, other spikes with positive values indicate the locked conformations of these molecules resulting from the formation of intramolecular and hydrogen bonds, as shown in Fig. 3 [44].





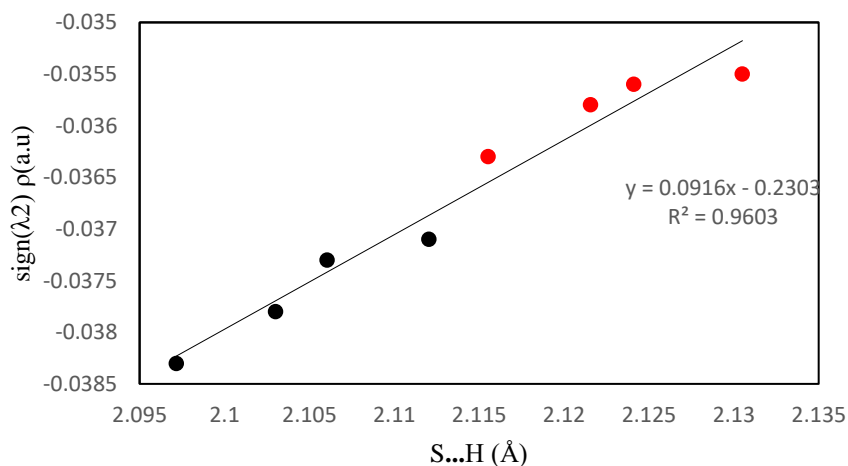
**Figure-3** NCI analysis of the studied molecules. (a) Plot of the electron density  $\{\text{sign}(\lambda^2)\rho\}$  vs the reduced gradient density. (b) Gradient isosurfaces. The data were obtained by evaluating  $\omega\text{B97XD}/6\text{-}311\text{++G(d,p)}$  density and gradient values on cubic grids. Isosurface of reduced density gradient = 0.5 (dotted line), (1, 3, 5 and 7 refer to aromatic substituents), (2, 4, 6 and 8 refer to aliphatic substituents).

Fig. 4 shows the relationship between  $\text{sign}(\lambda^2)\rho$  and  $\rho\text{BCP}$  with a linear regression coefficient  $R^2 = 0.97$ . An increase in the negative  $\text{sign}(\lambda^2)\rho$  value (close to  $-0.04$  a.u. or lower), as shown in Fig. 3, increases the  $\rho\text{BCP}$  value, indicating increased electron density in the bonding region of aromatic substituents (black circles). The aliphatic substituents decreased in  $\text{sign}(\lambda^2)\rho$  with decreasing  $\rho\text{BCP}$  (red circles). Hence, aromatic substituents confirm the existence of a strong and stable intramolecular hydrogen bond,  $\text{NH}\dots\text{S}$  than aliphatic substituents [45]. The correlation between the  $\text{sign}(\lambda^2)\rho$  and  $\rho\text{BCP}$  values facilitates the evaluation of the hydrogen bond strength and characteristics, which is crucial for comprehending the stability and reactivity of the enriched compounds [46]. NCI plots reveal that compounds with aromatic N-substituents have stronger hydrogen bonds (blue spikes at  $\sim -0.04$  a.u.), whereas aliphatic-substituted analogs have weaker connections (spikes near  $-0.03$  a.u.). In aliphatic chains, steric bulk may also obstruct the ideal H-bond form. These results validate the combined steric and electronic effects of substituents on the strength of hydrogen bonds.



**Figure-4** Relationship between  $\text{sign}(\lambda^2)\rho$  (a.u.) and  $\rho_{BCP}$  of H...S. (Black circles refer to aromatic substituents, red circles refer to aliphatic substituents).

The plot in Fig. 5 illustrates a positive association between the S...H hydrogen bond distance and the  $\text{sign}(\lambda^2)\rho$  (a.u.) value, with a linear regression  $R^2=0.96$ . A short S...H distance coupled with a significantly more negative sign of  $\text{sign}(\lambda^2)\rho$  and a short S...H bond length signifies a strong hydrogen bond resulting from close proximity and considerable electron density in the bonding region and related to aromatic substituents (black circles). While less negative values of  $\text{sign}(\lambda^2)\rho$  and longer S...H bond lengths indicate aliphatic substituents (red circles). By graphing these numbers (S...H bond length and  $\text{sign}(\lambda^2)\rho$ ), the strength and characteristics of hydrogen bonds within a certain system can be elucidated. Clusters of dots within designated ranges signify varying interaction strengths, facilitating the distinction between strong and weak hydrogen bonds [41].



**Figure -5** Relationships between the  $\text{sign}(\lambda^2)\rho$  (a.u.) and the S...H bond length (Å) (black circles refer to aromatic substituents, and red circles refer to aliphatic substituents).

## 4. Experimental

### 4.1 Materials

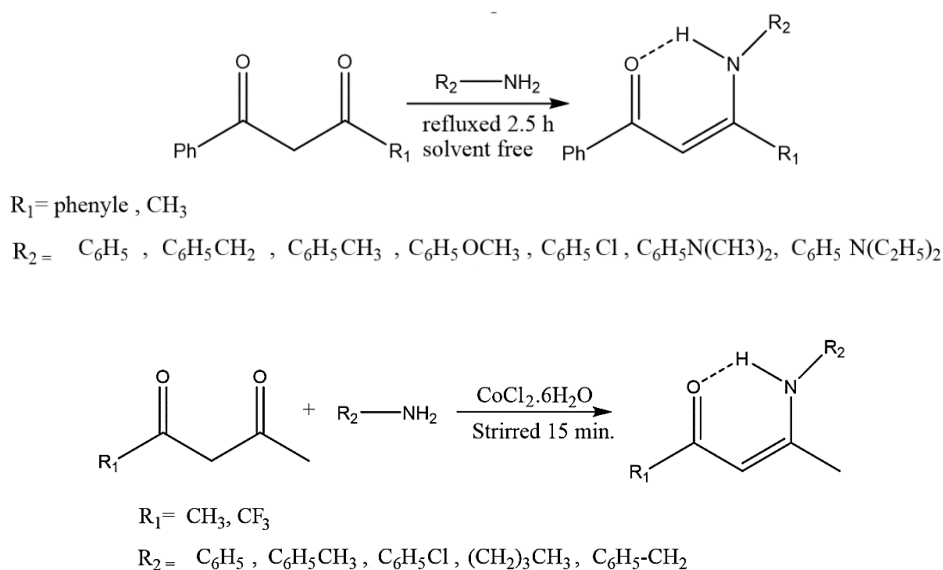
Commercial suppliers provided all of the chemicals, which were used without further purification. Additional purification has been applied to certain solvents.

### 4.2 Synthesis

A two-step procedure was used to synthesize enaminothiones, starting with the creation of enaminones and ending with their conversion to enaminothiones.

#### 4.2.1 Synthesis of enaminones

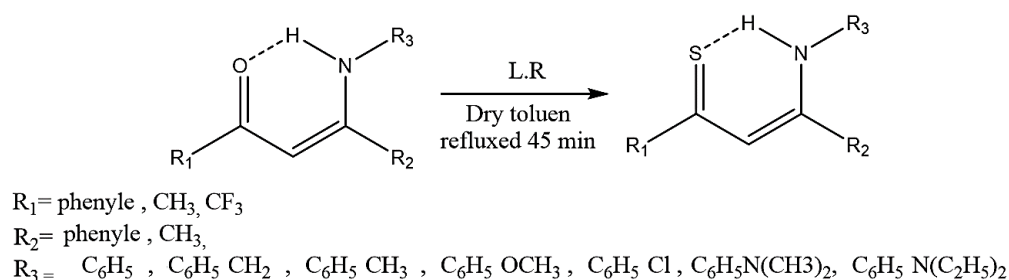
Enaminones were prepared by solvent-free mixing of various primary amines with dibenzoyl methane or benzoyl acetone. The mixture contained 10 mmol of amine and 10 mmol of  $\beta$ -diketone. The mixture was refluxed and stirred for 2.5 hours. As the mixture was monitored by TLC with a benzene:petroleum ether (2:1) eluent, it was cooled to room temperature. The product is recrystallized from ethanol and petroleum ether to obtain  $\beta$ -enaminones [47]. In another approach, acetylacetone or 1,1,1-trifluoroacetylacetone and benzylamine or butylamine were combined in a 1:1 molar ratio (10 mmol  $\beta$ -diketone: 10 mmol amine) with the addition of cobalt chloride (0.25 mmol  $\text{CoCl}_2 \cdot 6\text{H}_2\text{O}$ ) as a catalyst to produce  $\beta$ -enaminone. The solution was stirred for 15 minutes at room temperature and subsequently examined via thin-layer chromatography employing a solvent system of benzene and petroleum ether in a 2:1 ratio. The product was extracted with  $\text{CH}_2\text{Cl}_2$  ( $2 \times 30$  mL). Following three brine washes, the organic layers were dried with anhydrous sodium sulfate and recrystallized from ethanol and petroleum ether. The liquid products were further purified via vacuum distillation to produce  $\beta$ -enaminones [48]. Scheme 3 shows the process of preparing enaminone compounds.



**Scheme -3** enaminones synthesis

## 4.2.2 Synthesis of enaminothiones

To synthesize the enaminothiones, the enaminones described in section 4.2.1 were combined with Lawson's reagent at a 1:1 molar ratio, and toluene was dried for 45 minutes in an argon environment. Thin-layer chromatography (TLC) was employed to monitor the reactions involving benzene and petroleum ether in a 2:1 ratio. The product undergoes purification and separation via column chromatography utilizing a 2:1 benzene:petroleum ether eluent, as well as thin-layer chromatography [49]. Scheme 4 shows the process of preparing enaminothion compounds.



Scheme -4 enaminothion synthesis

## 4.2.3 Spectral and analytical data of synthesized compounds

**Compound 1:** 1,3-diphenyl-3-(phenylamino) prop-2-ene-1-thione

Red crystals; m.p. 162–163 °C; IR (KBr) NH broad band at 3150–3500  $\text{cm}^{-1}$ : C=N, 1595; C=C–H vinylic 660; C=S 785.  $^1\text{H}$  NMR (400 MHz,  $\text{CDCl}_3$ )  $\delta$  15.73 (s, 1H), 7.72 (dd,  $J = 7.6, 2.0$  Hz, 2H), 7.37–7.21 (m, 8H), 7.10 (t,  $J = 7.6$  Hz, 2H), 7.01 (t,  $J = 7.3$  Hz, 1H), 6.83 (dd,  $J = 7.5, 1.7$  Hz, 2H), 6.76 (s, 1H);  $^{13}\text{C}$  NMR (101 MHz,  $\text{CDCl}_3$ )  $\delta$  206.91, 162.52, 149.00, 138.05, 135.91, 130.19, 129.75, 129.05, 128.83, 128.45, 128.38, 128.12, 126.93, 125.79, 124.26, 114.74. EIMS  $m/z$  ( $\text{M}^+$ ): molecular ion 314.3, base peak 314.3.

**Compound 2:** 3-(Benzylamino)-1,3-diphenylprop-2-ene-1-thione

Pale red crystals; m.p. 162–163 °C; IR (KBr), NH broad band at 3250–3551  $\text{cm}^{-1}$ .  $^1\text{H}$  NMR (400 MHz,  $\text{CDCl}_3$ )  $\delta$  14.78 (s, 1H), 7.94–7.88 (m, 1H), 7.67 (dd,  $J = 7.4, 2.3$  Hz, 2H), 7.52–7.14 (m, 16H), 6.56 (d,  $J = 1.9$  Hz, 1H), 4.49 (d,  $J = 6.0$  Hz, 2H), 1.20 (s, 1H), 1.16 (dd,  $J = 12.0, 5.0$  Hz, 1H).  $^{13}\text{C}$  NMR (101 MHz,  $\text{CDCl}_3$ )  $\delta$  203.84, 185.81, 167.75, 148.76, 136.79, 135.56, 135.35, 132.54, 130.18, 129.41, 128.97, 128.87, 128.76, 128.00, 127.86, 127.45, 127.23, 127.16, 126.95, 113.44, 93.22, 49.04. EIMS  $m/z$  ( $\text{M}^+$ ): molecular ion, 330.1; base peak, 296.2.

**Compound 3:** 1-phenyl-3-(phenylamino) but-2-ene-1-thione

Brown red crystals; m.p., 125–127 °C. IR (KBr) NH broad band at 3250–3450  $\text{cm}^{-1}$ : C=N, 1545; C=C–H vinylic 695; C=S, 768.  $^1\text{H}$  NMR (400 MHz,  $\text{CDCl}_3$ )  $\delta$  15.82 (s, 2H), 7.74–7.66 (m, 4H), 7.39–7.31 (m, 4H), 7.30 (dd,  $J = 5.2, 1.9$  Hz, 6H), 7.27–7.16 (m, 6H), 6.65 (s, 2H), 2.16 (s, 6H), 1.18 (s, 1H).  $^{13}\text{C}$  NMR (101 MHz,  $\text{CDCl}_3$ )  $\delta$  203.63, 164.38, 148.70, 137.14, 129.45, 128.06, 127.28, 126.86, 125.35, 113.36, 29.74, 21.88. EIMS  $m/z$  ( $\text{M}^+$ ): molecular ion, 252.2; base peak, 252.2.

**Compound 4:** 3-(butylamino)-1-phenylbut-2-ene-1-thione

Brown crystals, m.p. 62—64 °C. IR (KBr), NH broad band 3441, C=N, 1600.9, C=C-H, 761, C=S, 890. <sup>1</sup>H NMR (400 MHz, CDCl<sub>3</sub>) δ 14.37 (s, 1H), 7.74–7.65 (m, 2H), 7.35–7.29 (m, 3H), 6.52 (d, *J* = 2.0 Hz, 1H), 3.50–3.41 (m, 2H), 2.17 (s, 2H), 1.74 (p, *J* = 7.1 Hz, 2H), 1.53 (dd, *J* = 16.3, 6.3 Hz, 1H), 1.27 (d, *J* = 10.3 Hz, 1H), 0.99 (t, *J* = 7.3 Hz, 3H), 0.92–0.81 (m, 0H). <sup>13</sup>C NMR (101 MHz, CDCl<sub>3</sub>) δ 199.70, 166.72, 148.81, 129.32 (d, *J* = 8.9 Hz), 128.97, 127.93, 126.83, 112.92, 77.28, 43.90, 31.21, 20.95, 20.28, 13.73. 233.2; EIMS *m/z* (*M*<sup>+</sup>): molecular ion 233, base peak 200.2.

**Compound 5:** 4-(Phenylamino) pent-3-ene-2-thione

Red crystals, m.p., 74—76 °C. IR (KBr), NH broad band 3458.3, C=N 1604., C=C-H, 735, C=S, 980. <sup>1</sup>H NMR (400 MHz, CDCl<sub>3</sub>) δ 15.51 (s, 1H), 7.42–7.33 (m, 3H), 7.14 (d, *J* = 8.5 Hz, 4H), 6.28 (d, *J* = 1.9 Hz, 2H), 3.00 (s, 1H), 2.62 (d, *J* = 1.8 Hz, 5H), 2.11 (s, 5H), 1.36 (s, 4H), 1.33–1.27 (m, 1H), 1.25 (s, 3H), 0.92–0.80 (m, 2H). <sup>13</sup>C NMR (101 MHz, CDCl<sub>3</sub>) δ 208.72, 163.15, 135.84, 132.83, 130.09, 129.56, 126.52, 113.98, 77.26, 39.17, 29.72, 21.39. EIMS *m/z* (*M*<sup>+</sup>): molecular ion 225.1, base peak 114.1.

**Compound 6:** 4-(butylamino) pent-3-ene-2-thione

Oil. <sup>1</sup>H NMR (400 MHz, CDCl<sub>3</sub>) δ 15.82 (s, 1H), 7.48 (dd, *J* = 8.5, 6.7 Hz, 2H), 7.40 (dd, *J* = 8.4, 6.3 Hz, 1H), 7.25 (d, *J* = 8.1 Hz, 2H), 6.80 (d, *J* = 2.4 Hz, 1H), 2.25 (s, 3H); <sup>13</sup>C NMR (101 MHz, CDCl<sub>3</sub>) δ 183.61, 183.29, 167.87, 135.90, 129.76, 128.39, 125.18, 121.79, 119.03, 112.41, 112.37, 112.34, 112.30, 21.75. EIMS *m/z* (*M*<sup>+</sup>): molecular ion 246.2, base peak 77.1.

**Compound 7:** 1,1,1-Trifluoro-4-(phenylamino) pent-3-ene-2-thione

Orange crystals, m.p. 56--58°C, IR (KBr); NH 3460.3, C=N, 1608.6--1595.3, C=S, 758.2, C=N, 692.4. <sup>1</sup>H NMR (400 MHz, CDCl<sub>3</sub>) δ 15.82 (s, 1H), 7.48 (dd, *J* = 8.5, 6.7 Hz, 2H), 7.40 (dd, *J* = 8.4, 6.3 Hz, 1H), 7.25 (d, *J* = 8.1 Hz, 2H), 6.80 (d, *J* = 2.4 Hz, 1H), 2.25 (s, 3H). <sup>13</sup>C NMR (101 MHz, CDCl<sub>3</sub>) δ 183.61, 183.29, 167.87, 135.90, 129.76, 128.39, 125.18, 121.79, 119.03, 112.36 (q, *J* = 3.6 Hz). EIMS *m/z* (*M*<sup>+</sup>): molecular ion 246.2, base peak 77.1.

**Compound 8:** 4-(butylamino)-1,1,1-trifluoropent-3-ene-2-thione

Oil. <sup>1</sup>H NMR (400 MHz, CDCl<sub>3</sub>) δ 14.68 (s, 1H), 7.44–7.28 (m, 9H), 6.67 (d, *J* = 2.1 Hz, 2H), 4.67 (d, *J* = 5.2 Hz, 4H), 2.21 (d, *J* = 1.2 Hz, 6H). <sup>13</sup>C NMR (101 MHz, CDCl<sub>3</sub>) δ 181.31, 180.99, 170.14, 134.50, 129.26, 128.46, 127.50, 122.05, 119.29, 112.32 (q, *J* = 3.7 Hz), 48.34, 29.89 – 29.31 (m), 21.09. EIMS *m/z* (*M*<sup>+</sup>): molecular ion 259.2, base peak 91.2.

## 5- Conclusion

This study confirms the significant effect of substituents on intramolecular hydrogen bonding in enaminothiones, with aromatic groups increasing the bond strength more effectively than aliphatic groups. The combination of DFT calculations, QTAIM, and NCI studies provided an exhaustive understanding of the electrical and geometric parameters influencing these interactions. These results establish a reliable foundation for predicting and enhancing hydrogen bonding characteristics in similar molecular systems. Future studies should investigate solvent effects, dynamic behavior, and various substituent modifications to increase our understanding of the fundamental characteristics of hydrogen bonding in enaminothiones.

## References

- [1] V. A. Usov and M. G. Voronkov, "β-Heterosubstituted α, β-Unsaturated Thioketones. Some Problems of Synthesis and Structure," *Sulfur Reports*, vol. 2, no. 2, pp. 39–75, 1982. [doi.org/10.1080/01961778208082426](https://doi.org/10.1080/01961778208082426)
- [2] K. T. Mahmudov and A. J. L. Pombeiro, "Resonance-assisted hydrogen bonding as a driving force in synthesis and a synthon in the design of materials," *Chemistry—A European Journal*, vol. 22, no. 46, pp. 16356–16398, 2016. [doi.org/10.1002/chem.201601766](https://doi.org/10.1002/chem.201601766)
- [3] D. Hornby, "Hydrogen bonding in biological structures: GA Jeffrey and W. Saenger, Springer-Verlag; Berlin, 1991; xiv+ 569 pages. DM 198.00. ISBN 3-540-50839-2," 1993, *No longer published by Elsevier*.
- [4] Y. Kelgokmen and M. Zora, "A new strategy for the synthesis of pyridines from N-propargylic β-enaminothiones," *Org Biomol Chem*, vol. 17, no. 9, pp. 2529–2541, 2019. [doi.org/10.1039/C8OB03180K](https://doi.org/10.1039/C8OB03180K)
- [5] R. S. Elias, Q. M. A. Hassan, B. A. Saeed, H. A. Sultan, P. E. Hansen, and C. A. Emshary, "Synthesis and study of nonlinear optical properties of an enaminoone derived from dibenzoylmethane and N,N-diethylaminoaniline," *Phys Scr*, vol. 99, no. 10, p. 105915, 2024. [DOI 10.1088/1402-4896/ad720c](https://doi.org/10.1088/1402-4896/ad720c)
- [6] I. Alkorta, I. Rozas, and J. Elguero, "Nonconventional hydrogen bonds," *Chem Soc Rev*, vol. 27, no. 2, pp. 163–170, 1998. [doi.org/10.1039/A827163Z](https://doi.org/10.1039/A827163Z)
- [7] R. Taylor and O. Kennard, "Crystallographic evidence for the existence of CH...O, CH...N and CH...Cl hydrogen bonds," *J Am Chem Soc*, vol. 104, no. 19, pp. 5063–5070, 1982. [doi.org/10.1021/ja00383a012](https://doi.org/10.1021/ja00383a012)
- [8] M. A. Viswamitra, R. Radhakrishnan, J. Bandekar, and G. R. Desiraju, "Evidence for OH...C and NH...C hydrogen bonding in crystalline alkynes, alkenes, and aromatics," *J Am Chem Soc*, vol. 115, no. 11, pp. 4868–4869, 1993. [doi.org/10.1021/ja00064a055](https://doi.org/10.1021/ja00064a055)
- [9] J. Ma, Y. Yang, X. Li, H. Sui, and L. He, "Mechanisms on the stability and instability of water-in-oil emulsion stabilized by interfacially active asphaltenes: Role of hydrogen bonding reconstructing," *Fuel*, vol. 297, p. 120763, 2021. [doi.org/10.1016/j.fuel.2021.120763](https://doi.org/10.1016/j.fuel.2021.120763)
- [10] C. J. Smallwood and M. A. McAllister, "Characterization of low-barrier hydrogen bonds. 7. Relationship between strength and geometry of short-strong hydrogen bonds. The formic acid–formate anion model system. An ab initio and DFT investigation," *J Am Chem Soc*, vol. 119, no. 46, pp. 11277–11281, 1997. [doi.org/10.1021/ja972517p](https://doi.org/10.1021/ja972517p)
- [11] S. J. Grabowski, "The bond valence model in analyzing H-bonds of crystal structures," *J Mol Struct*, vol. 552, no. 1–3, pp. 153–157, 2000. [doi.org/10.1016/S0022-2860\(00\)00474-9](https://doi.org/10.1016/S0022-2860(00)00474-9)
- [12] E. Espinosa, E. Molins, and C. Lecomte, "Hydrogen bond strengths revealed by topological analyses of experimentally observed electron densities," *Chem Phys Lett*, vol. 285, no. 3–4, pp. 170–173, 1998.
- [13] F. Fuster and S. J. Grabowski, "Intramolecular hydrogen bonds: the QTAIM and ELF characteristics," *J Phys Chem A*, vol. 115, no. 35, pp. 10078–10086, 2011. [doi.org/10.1021/jp2056859](https://doi.org/10.1021/jp2056859)
- [14] A. T. A. Boraie, M. Haukka, A. A. M. Sarhan, S. M. Soliman, and A. Barakat, "Intramolecular hydrogen bond, hirshfeld analysis, AIM; DFT studies of pyran-2,4-dione derivatives," *Crystals (Basel)*, vol. 11, no. 8, p. 896, 2021. [doi.org/10.3390/cryst11080896](https://doi.org/10.3390/cryst11080896)
- [15] A. Nowroozi, H. Roohi, M. Poorsargol, P. M. Jahani, H. Hajiabadi, and H. Raissi, "N...H...S and S...H...N intramolecular hydrogen bond in β-thioaminoacrolein: A quantum chemical study," *Int J Quantum Chem*, vol. 111, no. 12, pp. 3008–3016, 2011. <https://doi.org/10.1002/qua.22615>

- [16] S. Kumar Mishra and N. Suryaprakash, "Intramolecular hydrogen bonding involving organic fluorine: NMR investigations corroborated by DFT-based theoretical calculations," *Molecules*, vol. 22, no. 3, p. 423, 2017. <https://doi.org/10.3390/molecules22030423>
- [17] M. P. Johansson and M. Swart, "Intramolecular halogen-halogen bonds?," *Physical Chemistry Chemical Physics*, vol. 15, no. 27, pp. 11543–11553, 2013. DOI: [10.1039/C3CP50962A](https://doi.org/10.1039/C3CP50962A)
- [18] M. Kumar, I. Sadaf, J. Pamidighantam, Anamika, and S. Kumar, "Recent advance: Sulfur ylides in organic synthesis," *J Heterocycl Chem*, vol. 61, no. 1, pp. 29–70, 2024. <https://doi.org/10.1002/jhet.4736>
- [19] E. Arunan *et al.*, "Definition of the hydrogen bond (IUPAC Recommendations 2011)," *Pure and applied chemistry*, vol. 83, no. 8, pp. 1637–1641, 2011.
- [20] G. Hofacker, Y. Maréchal, M. Ratner, P. Schuster, G. Zundel, and C. Sandorfy, "The Hydrogen Bond Theory," *Schuster, P., Zundel, G., Sandorfy, C., Eds*, p. 297, 1976.
- [21] S. J. Grabowski, "An estimation of strength of intramolecular hydrogen bonds—ab initio and AIM studies," *J Mol Struct*, vol. 562, no. 1–3, pp. 137–143, 2001.
- [22] Gaussian 16, Revision C.01, M. J. Frisch, G. W. Trucks, H. B. Schlegel, G. E. Scuseria, M. A. Robb, J. R. Cheeseman, G. Scalmani, V. Barone, G. A. Petersson, H. Nakatsuji, X. Li, M. Caricato, A. V. Marenich, J. Bloino, B. G. Janesko, R. Gomperts, B. Mennucci, H. P. Hratchian, J. V. Ortiz, A. F. Izmaylov, J. L. Sonnenberg, D. Williams-Young, F. Ding, F. Lipparini, F. Egidi, J. Goings, B. Peng, A. Petrone, T. Henderson, D. Ranasinghe, V. G. Zakrzewski, J. Gao, N. Rega, G. Zheng, W. Liang, M. Hada, M. Ehara, K. Toyota, R. [23] F. Biegler-König and J. Schönbohm, "Update of the AIM2000-program for atoms in molecules," *J Comput Chem*, vol. 23, no. 15, pp. 1489–1494, 2002.
- [24] J. Cioslowski, A. Nanayakkara, and M. Challacombe, "Rapid evaluation of atomic properties with mixed analytical/numerical integration," *Chem Phys Lett*, vol. 203, no. 2–3, pp. 137–142, 1993.
- [25] J. R. Lane, S. D. Schröder, G. C. Saunders, and H. G. Kjaergaard, "Intramolecular hydrogen bonding in substituted aminoalcohols," *J Phys Chem A*, vol. 120, no. 32, pp. 6371–6378, 2016.
- [26] E. Espinosa and E. Molins, "Retrieving interaction potentials from the topology of the electron density distribution: the case of hydrogen bonds," *J Chem Phys*, vol. 113, no. 14, pp. 5686–5694, 2000.
- [27] T. Lu and F. Chen, "Multiwfn: A multifunctional wavefunction analyzer," *J Comput Chem*, vol. 33, no. 5, pp. 580–592, 2012.
- [28] W. Humphrey, A. Dalke, and K. Schulten, "VMD: visual molecular dynamics," *J Mol Graph*, vol. 14, no. 1, pp. 33–38, 1996.
- [29] D. L. Pavia, G. M. Lampman, G. S. Kriz, and J. R. Vyvyan, "Introduction to spectroscopy," 2015.
- [30] J. Zhuo, "NMR of Enaminones," *Magnetic resonance in chemistry*, vol. 35, no. 1, pp. 21–29, 1997.
- [31] M. Levien *et al.*, "Overhauser enhanced liquid state nuclear magnetic resonance spectroscopy in one and two dimensions," *Nat Commun*, vol. 15, no. 1, p. 5904, 2024.
- [32] D. Rusinska-Roszak, "Intramolecular O–H···O Hydrogen Bond Energy via the Molecular Tailoring Approach to RAHB Structures," *J Phys Chem A*, vol. 119, no. 15, pp. 3674–3687, 2015.
- [33] M. Jabłoński, "A critical overview of current theoretical methods of estimating the energy of intramolecular interactions," *Molecules*, vol. 25, no. 23, p. 5512, 2020.
- [34] J. Guo *et al.*, "Hydrogen bond geometries and proton tautomerism of homoconjugated anions of carboxylic acids studied via H/D isotope effects on <sup>13</sup>C NMR chemical shifts," *J Phys Chem A*, vol. 116, no. 46, pp. 11180–11188, 2012.
- [35] P. A. Frey, "Strong hydrogen bonding in molecules and enzymatic complexes," *Magnetic Resonance in Chemistry*, vol. 39, no. S1, pp. S190–S198, 2001.

- [36] I. Alkorta, F. Blanco, J. Elguero, J. A. Dobado, S. M. Ferrer, and I. Vidal, "Carbon··· carbon weak interactions," *J Phys Chem A*, vol. 113, no. 29, pp. 8387–8393, 2009.
- [37] J. A. Platts, J. Overgaard, C. Jones, B. B. Iversen, and A. Stasch, "First experimental characterization of a nonnuclear attractor in a dimeric magnesium (I) compound," *J Phys Chem A*, vol. 115, no. 2, pp. 194–200, 2011.
- [38] M. J. Z. Sagheb, L. Hokmabady, and A. Khanmohammadi, "A comprehensive investigation into the effect of substitution on electronic structure, charge transfer, resonance, and strength of hydrogen bond in 3-amino-propene thial and its analogous: A DFT calculation," *Chem. Rev. Lett*, vol. 6, p. 308, 2023.
- [39] I. Rozas, I. Alkorta, and J. Elguero, "Behavior of ylides containing N, O, and C atoms as hydrogen bond acceptors," *J Am Chem Soc*, vol. 122, no. 45, pp. 11154–11161, 2000.
- [40] J. Dutta, D. K. Sahoo, S. Jena, K. D. Tulsiyan, and H. S. Biswal, "Noncovalent interactions with inverted carbon: a carbo-hydrogen bond or a new type of hydrogen bond?," *Physical Chemistry Chemical Physics*, vol. 22, no. 16, pp. 8988–8997, 2020.
- [41] E. R. Johnson, S. Keinan, P. Mori-Sánchez, J. Contreras-García, A. J. Cohen, and W. Yang, "Revealing noncovalent interactions," *J Am Chem Soc*, vol. 132, no. 18, pp. 6498–6506, 2010.
- [42] J. Contreras-García *et al.*, "NCIPLOT: a program for plotting noncovalent interaction regions," *J Chem Theory Comput*, vol. 7, no. 3, pp. 625–632, 2011.
- [43] J. Contreras-García *et al.*, "NCIPLOT: a program for plotting noncovalent interaction regions," *J Chem Theory Comput*, vol. 7, no. 3, pp. 625–632, 2011.
- [44] P. R. Varadwaj, A. Varadwaj, and B. Jin, "Hexahalogenated and their mixed benzene derivatives as prototypes for the understanding of halogen··· halogen intramolecular interactions: New insights from combined DFT, QTAIM-, and RDG-based NCI analyses," *J Comput Chem*, vol. 36, no. 31, pp. 2328–2343, 2015.
- [45] C. Lefebvre, G. Rubez, H. Khartabil, J.-C. Boisson, J. Contreras-García, and E. Hénon, "Accurately extracting the signature of intermolecular interactions present in the NCI plot of the reduced density gradient versus electron density," *Physical Chemistry Chemical Physics*, vol. 19, no. 27, pp. 17928–17936, 2017.
- [46] P. Hobza and K. Müller-Dethlefs, *Noncovalent interactions: theory and experiment*, vol. 2. Royal Society of Chemistry, 2010.
- [47] N. A. Abood, Z. H. Aiube, and B. A. Saeed, "Spectroscopic Study of New Schiff Bases Derived from Dibenzoylmethane and Benzoylacetone," *Jour. Chem. Soc. Pak. Vol*, vol. 14, no. 2, 1992.
- [48] Z.-H. Zhang and J.-Y. Hu, "Cobalt (II) chloride-mediated synthesis of beta-enamino compounds under solvent-free conditions," *J Braz Chem Soc*, vol. 17, pp. 1447–1451, 2006.
- [49] W. A. A.-M. R. Sabah. Elyas. B. A. Saeed, "Preparation and properties of some enaminothiones derived from dibenzoylmethane," *J. Basrah studies*, , vol. 22, part 3, pp. 58–67, 1999.